

Numerical modelling of blood flow in a stented artery

G. Pontrelli¹ & G. Pedrizzetti²

¹*Istituto per le Applicazioni del Calcolo
CNR - Roma, Italy*

E-mail: g.pontrelli@iac.cnr.it

²*Dipartimento di Ingegneria Civile*

University of Trieste, Italy

E-mail: giannip@dic.univ.trieste.it

Abstract

A differential model of blood flow through a compliant vessel is first presented. A nonlinear viscoelastic constitutive equation for the wall is coupled with the 1D averaged fluid momentum equation. The nonlinear problem is solved by a finite difference method on a staggered grid and some numerical simulations are analyzed and discussed. To describe wave propagation disturbances due to a stent implantation, the effect of changes in elasticity properties along the vessel is also studied both with a full and with a perturbative method.

1 Introduction

Model studies of flows in liquid filled distensible tubes stem from the desire to understand the many aspects of the cardiovascular system in physiological and pathological states. Blood flow in arteries is dominated by unsteadiness and by wave propagation phenomena generated by the interaction of the blood with the arterial wall. The importance of the arterial mechanics is widely recognized in modelling hemodynamical problems. Some works have been carried out with the simplistic assumption that the vessel wall is linearly elastic and isotropic [1],[2]. The complex nature of biological tissues needs the development of nonlinear theories. Nonlinearities are not of great relevance for predictions of wave speed, but do influence the pressure and flow waveforms. This type of nonlinearity is a consequence of the curvature of the strain-stress function which shows that an artery

becomes stiffer as the distending pressure is raised. Some authors have shown that elasticity dominates the nonlinear mechanical properties of arterial tissues, whereas the vessel viscosity can be considered as a second order effect [3]. On the other hand, experimental studies indicate that the arterial material is viscoelastic and anisotropic [4]. In principle, viscoelastic dissipation of the vascular wall proves to be more important than viscous dissipation of the fluid. Actually, the latter can be neglected in a number of applications involving large blood vessels [1]. A review on the theoretical developments and new trends in arterial mechanics is given in [5].

Many theoretical and experimental formulations have been developed to describe the finite deformation and the nonlinear viscoelasticity of arteries in time dependent flows. A nonlinear constitutive relation for the vascular wall that depends on the Green strains has been introduced in [6] and a stability analysis on the saccular aneurysm evolution is presented in [7]. In the present work, such a model is extended to include the effect of the viscoelasticity of the solid wall. This is done in section 2, by letting the stress be a function of both the strain and strain rate. The inertia of the wall, even including the effective mass from the surrounding soft tissues, is negligible when compared with the elastic force because of low wall velocities [1], and it has been ignored.

Being interested in the pulse propagation phenomena, the assumption of a quasi-1D flow is a valid approach under the hypothesis that the wave amplitude is small and the wave length is long compared with the tube radius, so that the slope of the deformed wall remains small at all times [8]. We consider a homogeneous nonlinear viscoelastic tube filled with an incompressible fluid and all the quantities are assumed to vary in the axial direction while the equations have been integrated over the cross section. The mathematical formulation of the problem is given in section 3, and some numerical results are presented in section 4 for the unsteady flow sustained by pure oscillatory forcing, as a benchmark case. The flow dependence on the elasticity parameter and the mean pressure is shown. The effect of the elasticity parameter is related to the frequency of oscillations in the transient, while the influence of the viscosity parameter is to counterbalance possible instability phenomena. Despite the nonlinearity of the elastic part, the results are qualitatively similar to those obtained with a linear elastic relation studied in [9], because of the small arterial deformations. The effect of a varying elasticity coefficient (i.e. due to a stent insertion [10],[11]) on the flow dynamics is described in section 5.

The same analyses are also performed with a novel perturbative approach in section 6. This allows a substantial simplification of the system in the case of stiff arteries subjected to realistic dynamic loads.

2 The viscoelasticity of the vessel wall

The adequate mechanical characterization of blood vessels is an important prerequisite for a quantitative description of blood flow, mostly in wave propagation phenomena.

For an incompressible hyperelastic material, it is possible to define a strain-energy function W as a function of the stretch-ratio invariants I_1, I_2, I_3 : it represents the elastically stored energy per unit volume in terms of the strain variables and is a potential for the stress [12]. The problem of determining the form of the strain-energy function for biological materials has been examined from both theoretical and experimental points of view. A variety of mathematical expressions for W has been proposed in biomechanics, according to different materials and organic tissues, and their efficiency is tested in their ability to fit the experimental data over a wide range of strains. As pointed out by Fung [4] and other authors [5], the properties of vascular tissues are highly nonlinear. Some attempts to define a non-linear strain-energy density function for the arterial tissue are based on the static relationship between strains and elastic energy (see for example [4],[6],[13], and references therein).

Let us now consider the vessel wall modelled as an elastic axisymmetric membrane. This is a 2D thin shell with a negligible mass compared with that of the fluid contained within. The membrane is capable of deforming under the forces exerted by the fluid, is subject only to stresses in the tangential plane and has no bending stiffness. Let $(x_p(s), r_p(s))$ be the Lagrangian cylindrical coordinates of a particle P with s a parametric coordinate along the membrane. The strain-energy density function per unit area can be formulated as:

$$w = w(\lambda_1, \lambda_2)$$

where

$$\lambda_1 = \sqrt{\left(\frac{dr_p}{ds}\right)^2 + \left(\frac{dx_p}{ds}\right)^2} \quad \lambda_2 = \frac{r_p}{R_u} \quad (1)$$

are the principal deformation ratios in the meridional and circumferential directions and R_u is the undeformed radius. In this context, a constitutive strain-energy function modelling the mechanical properties of the arterial wall has been recently proposed [6],[7] as:

$$w = c_0 (e^Q - 1) \quad Q = c_1(E_1^2 + E_2^2) + 2c_3E_1E_2 \quad (2)$$

where c_0 is a material parameter having the same dimension as w (*force/length*), c_1, c_3 are nondimensional constants and $E_k = \frac{1}{2}(\lambda_k^2 - 1)$, $k = 1, 2$ are the principal Green strains. Once the form of w is specified, the mechanical properties are completely determined, being the stress components (averaged across the thickness) along the longitudinal and circumferential directions given by differentiation of w :

$$T_1(\lambda_1, \lambda_2) = \frac{\lambda_1}{\lambda_2} \frac{\partial w}{\partial E_1} = \frac{1}{\lambda_2} \frac{\partial w}{\partial \lambda_1} \quad T_2(\lambda_1, \lambda_2) = \frac{\lambda_2}{\lambda_1} \frac{\partial w}{\partial E_2} = \frac{1}{\lambda_1} \frac{\partial w}{\partial \lambda_2} \quad (3)$$

The former relations hold in the case of an incompressible and isotropic material, wherein principal directions of strain and stress coincide and express the property

that the instantaneous Young's modulus increases with the strain, but with a different amount in the two directions [5]. Note that c_0 acts as a scaling factor for T_1 and T_2 . The stresses T_1 and T_2 corresponding to the function (2) are reported in fig.1.

On the other hand, many authors have pointed out that the vessel walls are viscoelastic. Patel and Vaishnav [8] verified the existence of the arterial viscoelasticity through a dynamical experiment. Reuderink [2] found that a neglect of the viscoelasticity generates an underestimation of both phase velocity and damping. Generally, a viscoelastic wall model yields numerical results closer to physiological measurement than an elastic one, and a dissipative wall is more effective than a dissipative fluid in eliminating the high frequency oscillations. The damping resulting from viscoelasticity inhibits sharp peaks of the pressure and of flow pulses and leads to more realistic results when a comparison with dynamical experimental data is carried out [3].

The simplest generalization of eqn. (3), including a viscoelastic effect, is given the following linear strain rate-stress relationship:

$$\begin{aligned} T_1(\lambda_1, \lambda_2, \dot{\lambda}_1, \dot{\lambda}_2) &= \frac{1}{\lambda_2} \frac{\partial w}{\partial \lambda_1} + \gamma \left(\dot{\lambda}_1 + \frac{\dot{\lambda}_2}{2} \right) \\ T_2(\lambda_1, \lambda_2, \dot{\lambda}_1, \dot{\lambda}_2) &= \frac{1}{\lambda_1} \frac{\partial w}{\partial \lambda_2} + \gamma \left(\dot{\lambda}_2 + \frac{\dot{\lambda}_1}{2} \right) \end{aligned} \quad (4)$$

where $\gamma > 0$ is a wall viscosity coefficient and the dot denotes the time derivative [14].

Although the inertia of the membrane is neglected and a general theoretical framework is still lacking, in the model case studied here the simple functional strain-stress dependence in equations (4) takes into account the viscous effects of a material in time dependent motions and models the response of the arterial wall to the deformation and to the rate of deformation. In other words, equations (4) mean that the membrane does not respond instantaneously to forces, as a purely elastic body, but with a dissipative mechanism as a viscoelastic material.

3 The wall-fluid coupling

Owing to the small deformations of the vascular wall and to the unidirectional nature of waves in the arterial tree, a quasi-one dimensional model is adopted. Let us consider a homogeneous fluid of density ρ flowing in an axisymmetric distensible tube of circular cross section and let us introduce a set of nondimensional variables:

$$\begin{aligned} x &\rightarrow \frac{x}{R_0} & R &\rightarrow \frac{R}{R_0} & t &\rightarrow \frac{t U_0}{R_0} \\ u &\rightarrow \frac{u}{U_0} & p &\rightarrow \frac{p}{\rho U_0^2} & c_0 &\rightarrow \frac{c_0}{\rho R_0 U_0^2} \end{aligned}$$

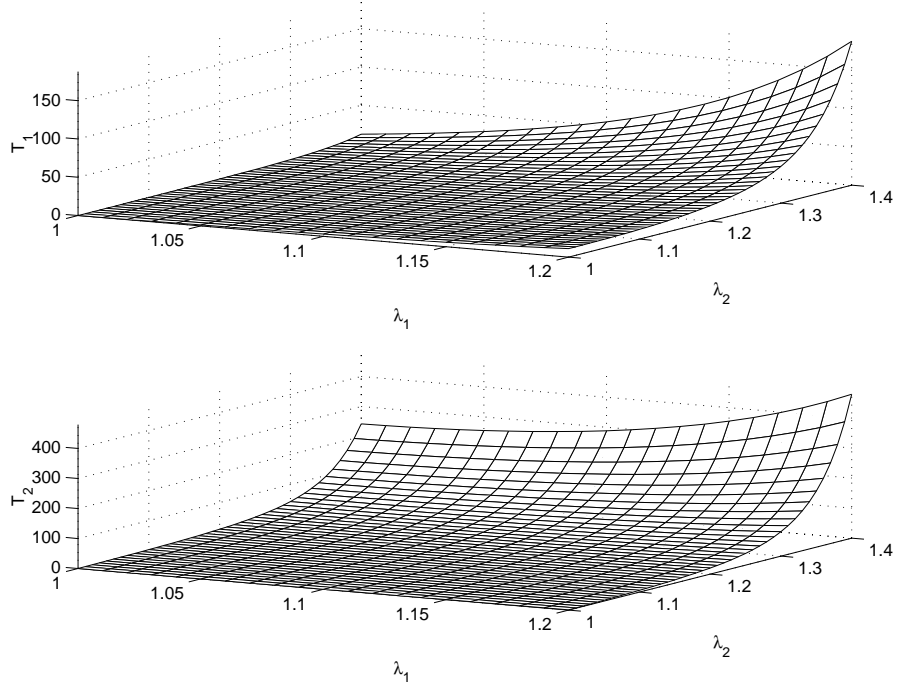


Figure 1: The strain-stress functions in eqn.(3) with $c_0 = 1$, $c_1 = 11.82$, $c_3 = 1.18$.

where x is the axial coordinate, R is the radius (with R_0 a reference constant radius), u is the averaged axial velocity (with U_0 a characteristic velocity), p denotes the transmural pressure and t the time.

Let us consider the 1D cross averaged momentum equation:

$$\frac{\partial u}{\partial t} + u \frac{\partial u}{\partial x} = -\frac{\partial p}{\partial x} + f \quad (5)$$

where f is a friction term [1]. This can be approximated by the friction term of the Poiseuille steady flow in a tube of radius R given by:

$$f \simeq -\frac{8u}{Re R^2} \quad (6)$$

with $Re = \frac{U_0 R_0}{\nu}$ the Reynolds number. As a consequence, the wall shear stress is approximated by:

$$\tau = \left. \frac{du}{dr} \right|_R \simeq -\frac{4u}{Re R} \quad (7)$$

In principle, the expressions (6) and (7) hold for a steady flow in a rigid tube, but they are considered acceptable for quasi steady flows and for small deformations ($R \approx R_0$) [2].

In a deformable tube the continuity equation is:

$$\frac{\partial R}{\partial t} + \frac{R}{2} \frac{\partial u}{\partial x} + u \frac{\partial R}{\partial x} = 0 \quad (8)$$

[1]. Because of its small inertia, the vessel wall is modelled as a membrane which deforms under the fluid forces and reaches an equilibrium state. Let us indicate by $R(x, t)$ and $S(x, t)$ the Eulerian counterparts of the Lagrangian coordinates of a particle of the membrane [14] (see previous section), for which the deformation ratios (1) can be expressed as

$$\lambda_1 = \sqrt{\frac{1 + R'^2}{S'^2}} \quad \lambda_2 = \frac{R}{R_u}$$

where the prime denotes x -derivative.

The fluid–membrane equilibrium equations in tangential and normal directions are provided [12]:

$$\begin{aligned} R'(T_1 - T_2) + RT'_1 &= \tau R(1 + R'^2)^{\frac{1}{2}} \\ \frac{-R''}{(1 + R'^2)^{\frac{3}{2}}} T_1 + \frac{1}{R(1 + R'^2)^{\frac{1}{2}}} T_2 &= p \end{aligned} \quad (9)$$

where τ is the shear stress exerted by the viscous fluid on the wall (cfr. (7)), non-dimensional stresses T_1 and T_2 are defined as in (4).

Since in wave propagation phenomena the dissipative effect of the blood viscosity is a minor effect [4], in the following simulations, an inviscid fluid is considered ($f \equiv 0$ in (5) and $\tau = 0$ in (9.1)).

The former equations (5), (8) and (9), together with the constitutive equations (4), model the nonlinear fluid-wall interaction and are solved in the segment between the two points $x = 0$ and $x = L$ which constitute the fictitious boundary of the differential problem. By considering the relevance of a pulsatile forcing in modelling vascular flows, two oscillatory boundary conditions are given at the extrema:

$$p(0, t) = p_{ref} + A_p \sin(2\pi S_t t) \quad u(L, t) = 0.5 + 0.5 \sin(2\pi S_t t) \quad (10)$$

where A_p is the nondimensional amplitude of pressure fluctuations, $S_t = \frac{R_0}{U_0 T_0}$ is the Strouhal number with T_0 the period of the incoming and outgoing waves, and U_0 is the peak velocity. Since the arterial wavelength is much larger than the length of a vessel, a phase shift and a difference in frequency at the inlet and outlet conditions (10) are small and they do not alter significantly the dynamics of the

system. Typical values of the dimensionless parameters in physiological regimes are:

$$p_{ref} = 40 \quad A_p = 10 \quad S_t = 0.01 \quad (11)$$

where the values of the nondimensional parameters are defined by letting: $R_0 = 0.5$ cm, $U_0 = 50$ cm/sec, $T_0 = 1$ s and minimum and maximum pressure 60 and 100 mmHg, respectively. Finally, the boundary conditions for S are imposed by considering an arbitrary value at $x = 0$ and a linear increasing at $x = L$, that is:

$$S(0, t) = 0 \quad S'(L, t) = 1$$

By evaluating the equation (9.2) at the boundary points (with the conditions $R' = R'' = 0$), we obtain two extra equations:

$$p R = T_2 \quad (\text{law of Laplace})$$

at $x = 0$ and $x = L$. The initial condition is chosen by considering an arbitrary configuration, obtained from the Poiseuille steady flow. Then the system is left to evolve being forced by an oscillating flow (see eqn. (10)).

4 Numerical method and results

The nonlinear equations describing the dynamics of the fluid-wall interaction are discretized by a second order finite difference method centered in space. Let us consider a sequence of $n + 1$ equispaced grid points $(x_i)_{i=0, \dots, n}$ with $x_0 = 0$ and $x_n = L$. The spatial discretization is obtained by evaluating membrane stresses, strains, and their time derivatives (see eqns. (4)) at n inner points $\xi_i = \frac{x_i + x_{i+1}}{2}$ of a staggered grid by considering averaged neighbouring quantities. On the other hand, equilibrium equations (9) and fluid equations (5)-(8) are computed at the $n - 1$ inner points x_i . The time discretization is based on the trapezoidal formula, in such a way the global scheme is of second order in space and time. The resulting nonlinear system is solved by a globally convergent Newton type method.

Nonlinear models turn out to be very sensitive to the many material parameters which characterize the specific flow problem. The reference values are fixed as $c_1 = 11.82$, $c_2 = 1.18$ (see [7]), $\gamma = 100$ and A_p and S_t as in (11). The other parameters have been chosen around some typical values to obtain results of physiological interest and varied in a typical range to test the sensitivity of the system to their perturbation. In particular we selected $5 \leq c_0 \leq 500$ and $1 \leq p_{ref} \leq 200$. The values of c_0 and p_{ref} are not independent: since the deformation is proportional to the ratio $\frac{p_{ref}}{c_0}$, it turns out that for $\frac{p_{ref}}{c_0} < \simeq 0.01$ the wall increases its stiffness and the numerical problem becomes harder. On the other hand, for a value of $\frac{p_{ref}}{c_0}$ too large, the system undergoes an unrealistic large deformation and the present model is not physically admissible. In all the experiments we selected $L = 8$, and the numerical parameters $\Delta x = 10^{-2}$ and $\Delta t = 5 \cdot 10^{-4}$. These values

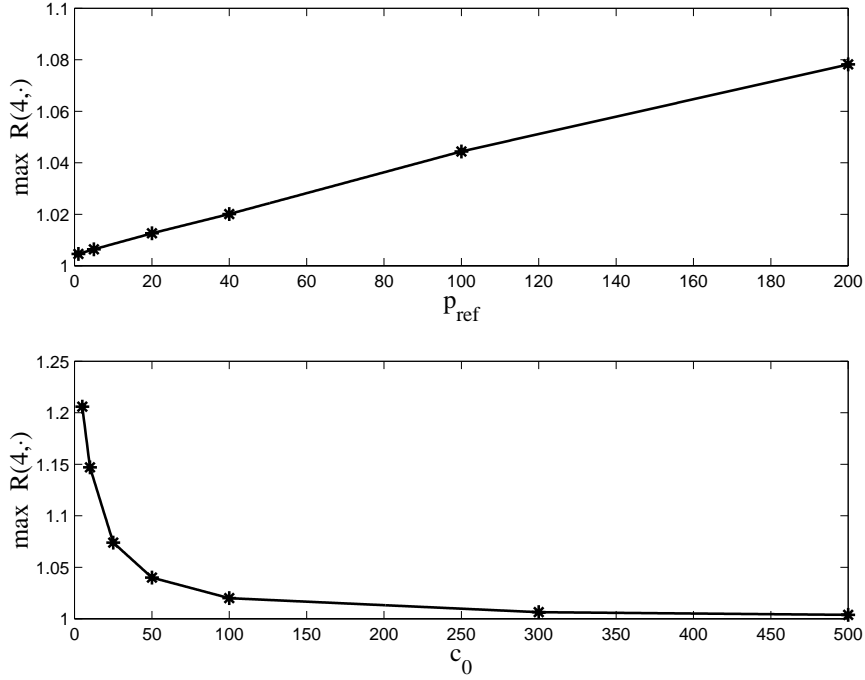


Figure 2: The maximum deformation at the center of the tube at varying mean pressure p_{ref} (above - $c_0 = 100$) and at varying elasticity coefficient c_0 (below - $p_{ref} = 40$). Starred points are results from simulations, continuous curves are obtained by a linear interpolation.

guarantee the numerical stability of the system for the set of parameters considered. The accuracy of the solution is controlled since the solution corresponding to a finer grid does not reveal a different structure or unresolved patterns.

After a short transient, the persistence of sinusoidal oscillations occurs with the same input frequency S_t with amplitude depending on the elasticity parameter (see below), while the frequency of the wave does not change with c_0, p_{ref} , as the natural elastic frequency, which is significantly higher, does [14],[15]. To avoid the effect due to the initial conditions, in the numerical simulations the transient has been dropped and only the solution after the second period is considered.

The value of the deformation is not influenced by γ : the viscous damping affects only waves of relatively short wavelength such as those of the natural oscillation, but is irrelevant for pulses of long wavelength such as those in the vascular system. The longitudinal deformation S exhibits very small changes compared to the radial one and is not discussed.

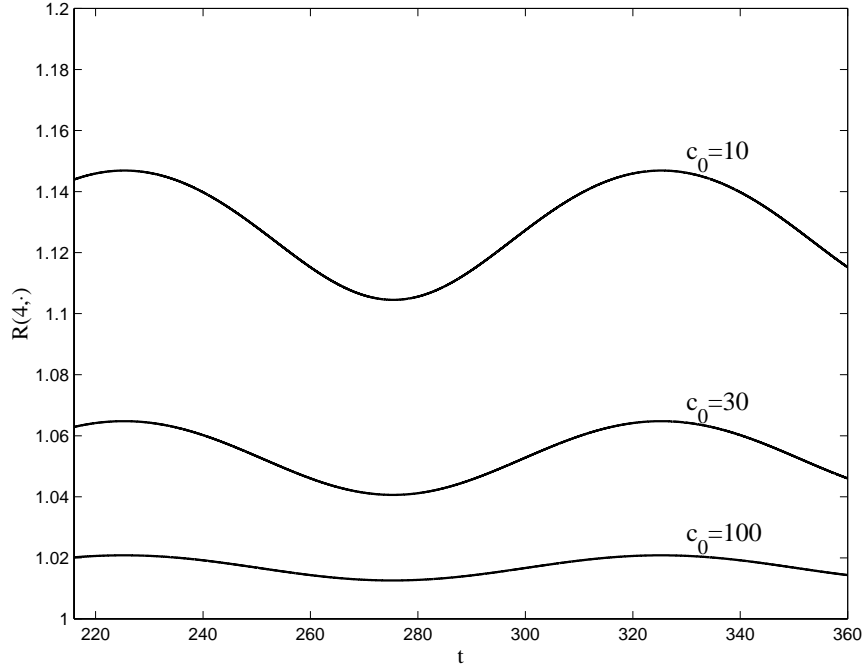


Figure 3: Deformation at the center of the tube for three values of the elasticity coefficient c_0 ($p_{ref} = 40$).

The dependence of the amplitude of the deformation on p_{ref} is nearly linear, while that on c_0 is inversely linear (fig. 2). Fig. 3 shows the evolution of R at the central point for three values of c_0 . The analysis of the radial velocity proves that the propagation features correspond to travelling waves which propagate along the tube. The present results agree qualitatively with those presented in [9] and show that the nonlinear character of the strain-stress function (see eqn. (3)) is responsible for minor changes with respect to the linear case. This is because of the small strains of the arterial motion (in the range of parameters considered: $\max_{x,t} \lambda_1 = 1.0003$ and $\max_{x,t} \lambda_2 = 1.2$).

5 The stent insertion

In many vascular pathologies, when the arterial lumen is extremely reduced, the stenting methodology has been successfully employed for a number of years. It is based on the implant of a tubular endoprosthesis (*stent*) to support the arterial wall (fig. 4).

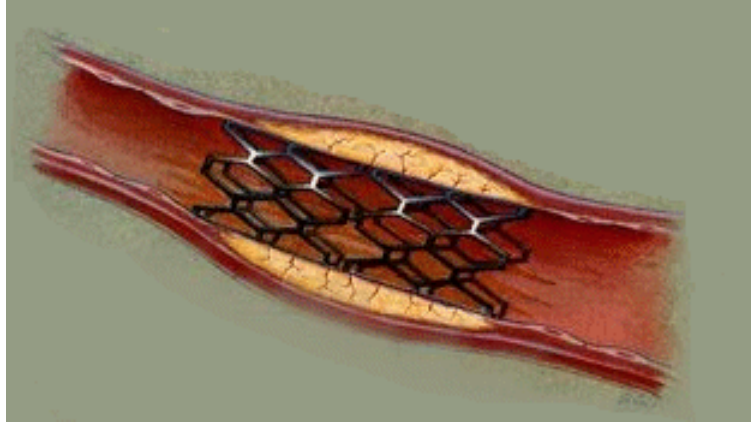


Figure 4: Implantation of a stent in a stenotic artery.

Despite its complex geometrical structure and a variety of mechanical characteristics, a stent can be schematically represented as a stiff cylindrical sleeve placed in the vessel to prevent or to correct narrowing of the section (i.e. stenosis) [10]. Although the stent implantation changes the geometry of the vessel and consequently induces important disturbances in the local flow [11],[16], a relevant effect in the wall-fluid interaction is the change of the compliance due to the sudden variation of the elasticity coefficient along the stent length.

Let us consider a stent of length 2σ centered in a point x^* and with elasticity coefficient $c_s > c_0$.

By considering the model (2), the elasticity parameter along the stented artery is given by:

$$c(x) = \begin{cases} c_s & \text{if } |x - x^*| < \sigma \\ c_0 & \text{otherwise} \end{cases}$$

and, to avoid a compliance mismatch between the relatively rigid stented segment and the distensible vessel, the elasticity coefficient is modelled by a continuous rapidly changing function:

$$c(x) = c_0 \left(1 + \delta e^{-\left(\frac{x - x^*}{\sigma}\right)^8} \right) \quad \delta = \frac{c_s - c_0}{c_0} \quad (12)$$

(for $c_s = c_0$ a uniform elasticity coefficient is recovered). The effect of a physiological local hardening or softening of an artery and the mechanical properties of stents can thus be roughly modelled by varying the value of δ and σ .

In the numerical simulations, we fixed $L = 8$, $x^* = 4$, $\sigma = 2$ (stent two diameters long), $c_0 = 100$ and we varied δ up to 9 in eqn. (12), with the wall viscosity coefficient $\gamma = 100$ unchanged. As expected, the maximum values of the

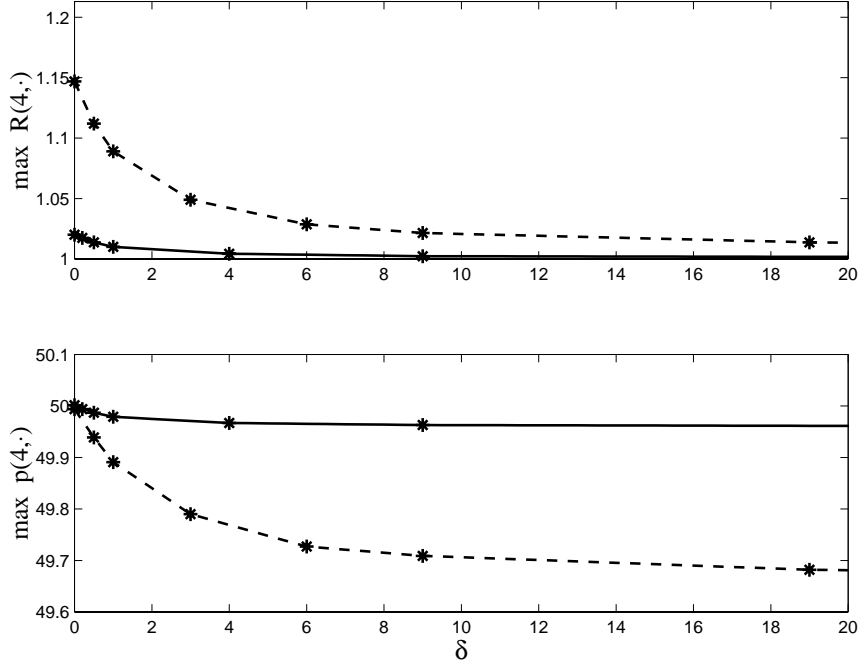


Figure 5: Variation of the variables at the centre of the stented artery with δ ($\sigma = 2, p_{ref} = 40$) - Solid line is for $c_0 = 100$, dashed line for $c_0 = 10$.

deformation and of the pressure at the centre of the tube are reduced with δ , and the asymptotic value consistent with a rigid wall is attained; this is shown in fig. 5, where the maximum deformation and pressure at the centre of the stent is shown at varying δ . On the other hand, the variation of the elasticity coefficient does not modify the frequency of the oscillation from that of the forcing.

The space-time evolution of the membrane radial velocity in a stented artery is depicted in fig. 6: a rapid variation of the stiffness corresponds to a similarly rapid variation of the membrane dynamics; it is also noticeable that the wave speed is increased when passing through the stent and is correspondingly decreased after crossing it.

6 A perturbative approach

When the vessel is sufficiently rigid and the wall deformations are small the previous method can be expressed in a simplified form by introducing a linearized, perturbative approach. This is an approximate method that derives from in vivo observations that the wall motion in large arteries is of relatively small entity even in response to significant pressure variations. In fact the deformation given by the pulsating unsteady pressure field is the dominant interaction in large arterial dis-

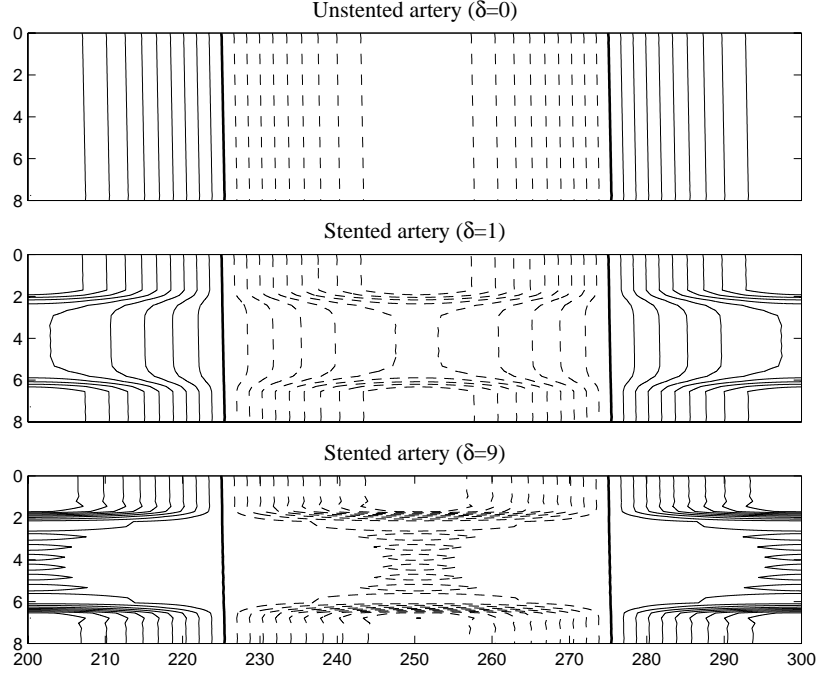


Figure 6: Space-time evolution of the membrane radial velocity over one period in a stented artery with $c_0 = 100$, for 3 values of δ ($\sigma = 2, p_{ref} = 40$). Thick line indicates the zero level, solid line positive levels, dashed line negative levels.

tricts of limited extent and self-excited flow-wall interactions either are absent or represent a second order effect. It is therefore possible to seek a solution of the fluid-wall system with a perturbative approach where the zeroth order solution is given by the flow in a rigid vessel, the first order correction gives the wall deformation and the induced flow modification, all without the need to solve the complex coupled problem [17].

In the case of small deformations the strain-stress relationship can be expressed in terms of linear elasticity. Linearization of equations (2)-(3) for small membrane deformations, gives:

$$T_2 = K (\lambda_2 - 1) \quad T_1 = \frac{1}{2} T_2;$$

where the second one comes from incompressibility, and the elasticity constant $K(x)$, i.e. the product of the Young modulus and membrane thickness in linear theory, corresponds to $K = 2c_0c_1$ in the linearization of the model (2)-(3). From

equation (9.2) the linearized wall radial equilibrium equation is written as:

$$R(x, t) - \bar{R}(x) = \frac{\bar{R}^2(x)}{K(x) \left(1 - \bar{R}'\bar{R}\right)} \left(p(x, t) - p_{ref}\right); \quad (13)$$

while the tangential equilibrium can be neglected to a first approximation. The reference geometry $\bar{R}(x)$ is the geometry in a long term equilibrium with the reference pressure p_{ref} , in absence of further knowledge and assuming still valid linear elasticity, it can be estimated a priori from $\bar{R}(x) = R_u \left(1 + \frac{p_{ref}}{K(x)}\right)$.

Equation (13) is a typical law of the wall (explicit relation between pressure and diameter), with properties varying along the vessel with the local elastic and geometrical characteristics.

The elasticity constant is usually, for stiff vessels, a large parameter that can be expressed as the ratio $K(x) = \frac{f(x)}{\varepsilon}$ where $f(x)$ is an order one possible modulation and ε is a small parameter which represents the characteristic compliance value. In correspondence of the model (12) we adopt $f(x) = \frac{2c(x)c_1}{c_0}$ and the small parameter $\varepsilon = \frac{1}{c_0}$.

Based on the presence of the small parameter ε we propose a perturbative approach to the interacting wall-fluid system. All variables are expressed in series of ε , taking a first order approximation which neglects $O(\varepsilon^2)$ terms, we express

$$\begin{aligned} R(x, t) &= \bar{R}(x) + \varepsilon \Delta R^{(1)}(x, t) \\ u(x, t) &= u^{(0)}(x, t) + \varepsilon u^{(1)}(x, t) \\ p(x, t) &= p^{(0)}(x, t) + \varepsilon p^{(1)}(x, t) \end{aligned} \quad (14)$$

the $O(\varepsilon^0)$ terms represent the flow in a rigid vessel whereas the $O(\varepsilon^1)$ terms are the first correction due to the wall elasticity.

The continuity equation (8) and the momentum equations (5) for the order zero variables become, respectively:

$$\begin{cases} \frac{\partial}{\partial x} \left(u^{(0)} \bar{R}^2\right) = 0 \\ \frac{\partial p^{(0)}}{\partial x} = -\frac{\partial u^{(0)}}{\partial t} - u^{(0)} \frac{\partial u^{(0)}}{\partial x} \end{cases} \quad (15)$$

which can be solved one after the other by an explicit space integration starting from the location where the boundary conditions are specified. By substituting eqns. (14) into the linearized equilibrium eqn. (13), the wall deformation is given at the first order with an explicit expression in terms of the order zero pressure

$$\Delta R^{(1)}(x, t) = \frac{\bar{R}^2(x)}{f(x) \left(1 - \bar{R}'\bar{R}\right)} \left(p^{(0)}(x, t) - p_{ref}\right) \quad (16)$$

The order one solutions can again be evaluated explicitly in the perturbative cascade. The order one velocity is found from a space integration of the continuity equation (8) after only first order terms in ε are retained

$$\frac{\partial}{\partial x} \left(u^{(1)} \bar{R}^2 \right) = -2\bar{R} \left(\frac{\partial}{\partial t} \Delta R^{(1)} + u^{(0)} \frac{\partial}{\partial x} \Delta R^{(1)} + \frac{\Delta R^{(1)}}{2} \frac{\partial u^{(0)}}{\partial x} \right) \quad (17)$$

and the pressure correction can then be evaluated similarly from the conservation of momentum. The system (15)-(17) is solved numerically without the need to specify the actual value of c_0 which is regarded as the perturbative parameter.

Results obtained from the two presented techniques have been compared. Figure 7 is the analogue of fig.5 (upper) and reports results obtained with a perturbation method. For $c_0 = 100$ the curves are almost indistinguishable and the asymptotic technique is revealed as being quite accurate.

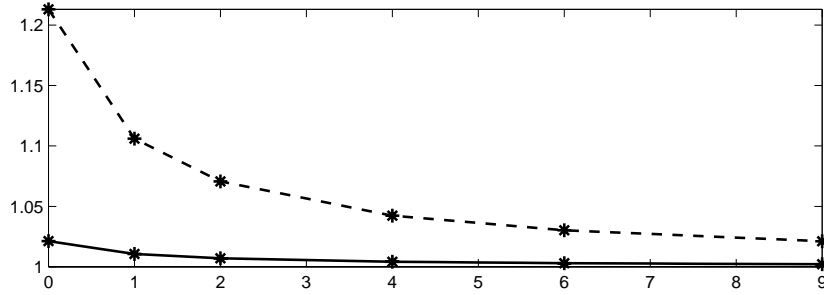


Figure 7: As in fig. 5a (upper). Results are obtained from the perturbation method with the same parameters.

For softer arteries, as for $c_0 = 10$, the linear elasticity model yields an over-estimation of the deformation because it does not include the changing stiffness of the nonlinear model; however the error is reduced at larger δ .

Figure 8 shows the same results as in fig. 6, with the present simplified approach. Again, a linearized elastic model is adequate to reproduce the same behaviour for $c_0 = 100$ and the illustrations show that the wall dynamics is well captured by the perturbative method in such a case.

7 Conclusions

In order to model the blood flow through a stented artery, the hemodynamics of the pulsatile flow in an arterial segment has been studied in relation to the viscoelastic properties of the vessel wall. The fluid-wall interaction is described by a 1D model and is expressed by a set of four nonlinear partial differential equations. The dependence on the many parameters has been pointed out in the case of oscillatory flow and the influence of some of them in a case of clinical relevance has

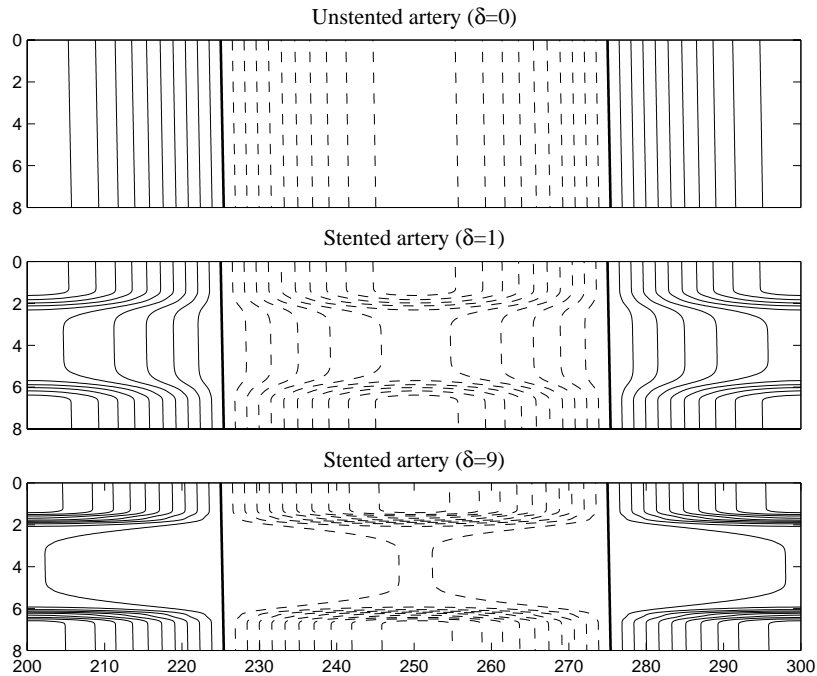


Figure 8: As in fig. 6. Results are obtained from the perturbation method with the same parameters, contour levels and steps.

been examined. For small arterial deformations a perturbative method has been shown to correctly approximate the full nonlinear model. Therefore the technique can be employed to extract simple information for the immediate estimates of relevant quantities. Finally, the geometrical, physical and biomechanical parameters need to be carefully identified according to a specific flow problem.

References

- [1] Pedley T.J., *The fluid mechanics of large blood vessels*, Cambridge University Press, 1980.
- [2] Reuderink P.J., Hoogstraten H.W., Sipkema P., Hillen B. & Westerhof N., Linear and nonlinear one-dimensional model of pulse wave transmission at high Womersley numbers, *J. Biomech.*, **22** (8/9), pp. 819–827, 1989.
- [3] Horsten J.B., van Steenhoven A.M. & van Dongen A.A., Linear propagation of pulsatile waves in viscoelastic tubes, *J. Biomech.*, **22**, pp. 477–484, 1989.
- [4] Fung Y.C., *Biomechanics: Mechanical properties of living tissues* (2nd Ed.), Springer-Verlag, New York, 1993.
- [5] Humphrey J.D., Mechanics of the arterial wall: review and directions, *Crit.*

- Review in Biomed. Engineering*, **23** (1/2), pp. 1–162, 1995.
- [6] Kyriacou S.K. & Humphrey J.D., Influence of size, shape and properties on the mechanics of axisymmetric saccular aneurysms, *J. Biomech.*, **29** (8), pp. 1015–1022, 1996.
 - [7] Shah A.D. & Humphrey J.D., Finite strain elastodynamics of intracranial saccular aneurysms, *J. Biomech.*, **32**, pp. 593–599, 1999.
 - [8] Patel D.J. & Vaishnav R.N., *Basic Hemodynamics and its role in disease processes*, University Park Press, Baltimore, 1980.
 - [9] Pontrelli G., *A mathematical model of flow in a liquid-filled viscoelastic tube*, *Med. Biol. Eng. Comput.*, **40** (5), pp. 550–556, 2002.
 - [10] Xu X.Y. & Collins M.W., Flow pattern in stented arteries, *Internal Medicine*, **5** (1), pp. 29–32, 1997.
 - [11] Auricchio F., Di Loreto M. & Sacco E., Finite-element analysis of a stenotic artery revascularization through a stent insertion, *Comp. Meth. in Biomech. and Biom. Eng.*, **4**, pp. 249–263, 2001.
 - [12] Green A.E. & Adkins J.E., *Large elastic deformations*, Clarendon Press, Oxford, 1960.
 - [13] Demiray H., A quasi-linear constitutive relation for arterial wall material, *J. Biomech.*, **29** (8), pp. 1011–1014, 1996.
 - [14] Pedrizzetti G., Fluid flow in a tube with an elastic membrane insertion, *J. Fluid Mech.*, **375**, pp. 39–64, 1998.
 - [15] Pontrelli G., Nonlinear problems in arterial flows, *Nonlinear Analysis*, **47**, pp. 4905–4915, 2001.
 - [16] Peacock J., Hankins S., Jones T. & Lutz R., Flow instabilities induced by coronary artery stents: assessment with an in vivo pulse duplicator, *J. Biomech.*, **28**, pp. 17–26, 1995.
 - [17] Pedrizzetti G., Domenichini F., Tortoriello A. & Zovatto L., Pulsatile flow inside moderately elastic arteries, its modelling and effects of elasticity, *Comp. Meth. in Biomech. and Biom. Eng.*, **5** (3), pp.219–231, 2002.